Journal of Computational Physics 229 (2010) 5457–5464

Contents lists available at ScienceDirect

Journal of Computational Physics

journal homepage: www.elsevier.com/locate/jcp

A splitting scheme for highly dissipative smoothed particle dynamics

S. Litvinov [a], M. Ellero [a,b], X.Y. Hu [a,*], N.A. Adams [a]

[a] Lehrstuhl für Aerodynamik, Technische Universität München, 85748 Garching, Germany
[b] Departamento de Física Fundamental, UNED, Apartado 60141, 28080 Madrid, Spain

ARTICLE INFO

Article history:
Received 29 September 2009
Received in revised form 1 March 2010
Accepted 17 March 2010
Available online 30 March 2010

Keywords:
Smoothed particle hydrodynamics
Smoothed dissipative particle dynamics
Operator splitting
Schmidt number

ABSTRACT

Smoothed particle dynamics refers to Smoothed Particle Hydrodynamics (SPH) when simulating macroscopic flows and to Smoothed Dissipative Particle Dynamics (SDPD) when simulating mesoscopic flows. When the considered flow is highly dissipative, this otherwise very attractive method faces a serious time-step limitation. This difficulty, known in literature as Schmidt number problem for Dissipative Particle Dynamics (DPD), prevents the application of SDPD for important cases of liquid micro-flows. In this paper we propose a splitting scheme which allows to increase significantly the admissible time-step size for SPH and SDPD. Macroscopic and mesoscopic validation cases, and numerical simulations of polymer in shear flows suggest that this scheme is stable and accurate, and therefore efficient simulations at Schmidt numbers of order $O(10^6)$ are possible.

1. Introduction

Smoothed particle dynamics is a fully Lagrangian, grid free method, where a smoothing kernel is introduced to approximate functions and their spatial derivatives from data carried by neighboring particles. It is referred to as Smoothed Particle Hydrodynamics (SPH) when simulating macroscopic flows [1], and as Smoothed Dissipative Particle Dynamics (SDPD) when simulating mesoscopic flows [2,3]. SDPD also can be viewed as a modification of Dissipative Particle Dynamics (DPD), a popular mesoscopic particle-based method [4]. Compared to DPD, in SDPD transport coefficients can be prescribed as input parameters rather than being an indirect result of other model parameters. Thermal fluctuations can be introduced adaptively according to the size of the fluid particles.

When the smoothed particle dynamics method is used to simulate low-Reynolds-number and mesoscopic liquid flows, the time-step size limit for stable time integration is usually determined by the viscous effects as such flows are highly dissipative. Specifically, this issue is referred to as Schmidt number problem in DPD [5,6] and obviously also applies to SDPD. The Schmidt number is defined as the ratio of momentum diffusivity (viscosity) and mass diffusivity

$$\mathrm{Sc} = \frac{\mu}{D\rho}, \tag{1}$$

where μ is dynamic viscosity, ρ is density and D is the diffusion coefficient. Typical Sc number achieved by SDPD and DPD simulations are of order $O(1)$, which is similar to that of a gas rather than a liquid with Sc $\sim O(10^3)$.

Peters [7] suggested that the diffusion coefficient D appearing in the definition of Sc refers to the molecular diffusivity and therefore is an ill-defined quantity for coarse-grained systems. Accordingly, one would not need to achieve realistically large Sc to capture correct hydrodynamic interactions [8–10]. However, it has been pointed out by Groot and Warren [11] that in order to achieve a realistic liquid behavior it is essential to recover the correct magnitude of Sc in DPD simulation. Furthermore, it was observed by Symeonidis et al. [5,12] that an agreement between simulations and experiments with

* Corresponding author.
E-mail address: Xiangyu.Hu@aer.mw.tum.de (X.Y. Hu).

0021-9991/$ - see front matter © 2010 Elsevier Inc. All rights reserved.
doi:10.1016/j.jcp.2010.03.040

respect to the non-equilibrium properties of a DNA molecule in a shear flow requires Sc numbers with a magnitude of that for a liquid.

For increasing Sc in DPD simulation one could generate a higher viscosity by increasing the stiffness of the conservative force or the number density of DPD particles, or the dissipative force. Since the represented length scale decreases with the increase of the former two quantities, these approaches contradict the intended coarse-graining property of the DPD method. Therefore, a common approach for increasing Sc is to increase the magnitude of the dissipative force. However, if the DPD particle velocity is updated explicitly, as in the traditional velocity-Verlet method [11], the time integration requires a very small, computationally inefficient time-step size to achieve correct equilibrium properties. To cope with this difficulty, Pagonabarraga et al. [13] have proposed an iterative method where the particle velocity is updated implicitly. However, it is found that such a method is not very practical due to large computational cost. Lowe [14] developed an alternative DPD method where the dissipative and random forces of the traditional DPD method are replaced by a pairwise momentum-conservative Andersen thermostat, which relates the resulting viscosity to a prescribed random relaxation parameter. Due to the Andersen thermostat the method recovers the correct kinetic temperature independently of the time-step size and can be used for simulating a DPD fluid with high Sc. One issue of this method is that the deterministic dissipative term in DPD is replaced by a stochastic term which may lead to strong spatial–temporal fluctuations of the dissipation rate when the time-step size is large.

More recently, a splitting scheme for DPD was proposed by Shardlow [15]. While updating the contribution of the conservative force explicitly, similarly to that of Lowe's method, this method updates the contributions of the dissipative and random forces in pairwise fashion. By this procedure the original DPD formulation of dissipative and random forces is preserved. Nikunen et al. [16] showed that the accuracy and performance of Shardlow's scheme is superior to that of several other schemes commonly used in DPD. However, compared to that of Lowe's method, the kinetic temperature is still significantly overestimated when a large time-step size is used. It is interesting to note that in an earlier work of Monaghan [17] a splitting scheme similar to that of Shardlow [15] was described for handling the drag force on dust particles when modeling dust-gas flow with an SPH method. To recover very large drag coefficients the pairwise interactions are computed by sweeping over all the dust-gas particle pairs several times. Although this method originally has been developed for a drag-force model an extension to general viscous flows appears to be straightforward.

In this work we present a splitting scheme for the smoothed particle dynamic method which can be viewed as a combination and extension of Shardlow's and Monaghan's schemes. The scheme achieves significantly larger time-step sizes than is possible by the standard predictor–corrector and velocity-Verlet schemes, and can be applied for general macroscopic and mesoscopic viscous flows. To demonstrate the robustness and efficiency of the method, a number of validation tests and examples for macroscopic and microscopic flows are given.

2. SPH and SDPD

For SPH the temporal evolution of discrete-particle location and properties is given by

$$\frac{d\mathbf{r}_i}{dt} = \mathbf{v}_i, \tag{2a}$$

$$\rho_i = m_i \sum_j W_{ij} = m_i \sigma_i, \tag{2b}$$

$$\frac{d\mathbf{v}_i}{dt} = -\frac{1}{m_i}\sum_j \left(\frac{p_i}{\sigma_i^2} + \frac{p_j}{\sigma_j^2}\right)\frac{\partial W_{ij}}{\partial r_{ij}}\mathbf{e}_{ij} + \frac{\mu}{m_i}\sum_j \left(\frac{1}{\sigma_i^2} + \frac{1}{\sigma_j^2}\right)\frac{\mathbf{v}_{ij}}{r_{ij}}\frac{\partial W_{ij}}{\partial r_{ij}}, \tag{2c}$$

representing a Lagrangian discretization of the Navier–Stokes equations for isothermal, weakly compressible flow [3]. Here, $\mathbf{e}_{ij}$ and r_{ij} are the normalized vector and distance from particle i to particle j, respectively. $\mathbf{r}_i$,$\mathbf{v}_i$,m_i,ρ_i and p_i are position, velocity, mass, density and pressure of a particle i, respectively. σ_i is the inverse of particle volume, and $W_{ij} = W(r_{ij},h)$ is a kernel function with smoothing length h. An isothermal equation of state is given as

$$p = p_0\left(\frac{\rho}{\rho_0}\right)^{\gamma} + b, \tag{3}$$

where p_0,ρ_0, b and γ are parameters which may be chosen based on a scale analysis so that the density variation is less than a given value, usually 1% [18].

Within the SDPD formulation [2] Eq. (2) presents the deterministic part of the particle dynamics. Using the GENERIC formalism [19,20] thermal fluctuations can be taken into account by postulating the following expressions for mass and momentum fluctuations

$$d\tilde{m}_i = 0, \tag{4a}$$

$$d\widetilde{\mathbf{P}}_i = \sum_j B_{ij} d\overline{\overline{W}}_{ij}\mathbf{e}_{ij}, \tag{4b}$$

where $\overline{\overline{dW}}_{ij}$ is the traceless symmetric part of a tensor of independent increments of a Wiener process, and B_{ij} is defined as

$$B_{ij} = \left[-4k_B T\mu \left(\frac{1}{\sigma_i^2} + \frac{1}{\sigma_j^2} \right) \frac{1}{r_{ij}} \frac{\partial W}{\partial r_{ij}} \right]^{1/2}, \tag{5}$$

where k_B is Boltzmann constant and T is a prescribed fluid temperature [3]. Note that the evolution equations for SPH and SDPD can be written in a generic form as

$$d\mathbf{v}_i = \frac{1}{m_i} \left(\mathbf{F}_i^C dt + \mathbf{F}_i^D dt + d\widetilde{\mathbf{P}}_i \right), \tag{6a}$$

$$d\mathbf{r}_i = \mathbf{v}_i dt, \tag{6b}$$

where $\mathbf{F}_i^C = \sum_j \left(\frac{p_i}{\sigma_i^2} + \frac{p_j}{\sigma_j^2} \right) \frac{\partial W_{ij}}{\partial r_{ij}} \mathbf{e}_{ij}$ is the conservative force and the $\mathbf{F}_i^D = \sum_j \left(\frac{1}{\sigma_i^2} + \frac{1}{\sigma_j^2} \right) \frac{\mathbf{v}_{ij}}{r_{ij}} \frac{\partial W_{ij}}{\partial r_{ij}}$ is the dissipative force as given by the right hand side of Eq. (2c)

When Eq. (6) is integrated by standard explicit schemes, such as a predictor–corrector scheme for SPH or velocity-Verlet for SDPD, the time-step size is constrained by the Courant–Friedrichs–Lewy (CFL) condition

$$\Delta t \leqslant \Delta t_c = 0.25 \frac{h}{c}, \quad c = 10 V_{max}, \tag{7}$$

where c is a chosen speed of sound, V_{max} is the maximum flow speed, and

$$\Delta t \leqslant \Delta t_\mu = 0.125 \frac{\rho h^2}{\mu}. \tag{8}$$

Since typical micro-fluidic problems are characterized by very small Reynolds numbers and dominated by viscous effects [18], it is desirable to relax the viscous time-step limit $\Delta\, t_\mu$ for numerical simulation.

3. Splitting scheme

The fundamental concept of the splitting approach is that the contribution of the conservative force is updated separately from that of the dissipative and the random forces (time-splitting). The latter are updated implicitly in a pairwise fashion (operator-splitting).

The splitting scheme can be described as follows. First, an intermediate velocity $\tilde{\mathbf{v}}_i$, due to dissipative and random forces, is obtained in a pairwise fashion by sweeping over all pairs of neighboring particles a certain number of times (N_s). For a specific particle pair their velocities are updated according to the following two-step procedure. The first step is explicit, and can be written as

$$\mathbf{v}_i' = \mathbf{v}_i + \frac{1}{2} \frac{1}{m_i} \mathbf{F}_{ij}^D \Delta t_{N_s} + \frac{1}{2} \frac{d\widetilde{\mathbf{P}}_{ij}}{m_i}, \tag{9a}$$

$$\mathbf{v}_j' = \mathbf{v}_j - \frac{1}{2} \frac{1}{m_j} \mathbf{F}_{ij}^D \Delta t_{N_s} - \frac{1}{2} \frac{d\widetilde{\mathbf{P}}_{ij}}{m_j}, \tag{9b}$$

where $\Delta t_{N_s} = \Delta t / N_s$ is the sub-time-step size, and $d\widetilde{\mathbf{P}}_{ij}$ is the momentum fluctuation between the particle pair. The second step is implicit, and can be written as

$$\tilde{\mathbf{v}}_i = \mathbf{v}_i' + \frac{1}{2} \frac{1}{m_i} \widetilde{\mathbf{F}_{ij}^D} \Delta t_{N_s} + \frac{1}{2} \frac{d\widetilde{\mathbf{P}}_{ij}}{m_i}, \tag{10a}$$

$$\tilde{\mathbf{v}}_j = \mathbf{v}_j' - \frac{1}{2} \frac{1}{m_j} \widetilde{\mathbf{F}_{ij}^D} \Delta t_{N_s} - \frac{1}{2} \frac{d\widetilde{\mathbf{P}}_{ij}}{m_j}, \tag{10b}$$

where $\tilde{\mathbf{v}}_i, \tilde{\mathbf{v}}_j$ on both sides of Eq. (10) are updated simultaneously. Monaghan [17] used an updating similar to Eq. (10), where no thermal fluctuations are present and $\widetilde{\mathbf{F}_{ij}^D}$ is given by a drag-force model rather than by an expression for a general viscous force such as used here, see Eq. (2). As there are only two unknowns for two equations the solution of Eq. (10) is straightforward and stable, independently of Δt_{N_s}. For $\mu \to \infty$ the resulting velocities at the end of a single pair-update are

$$\tilde{\mathbf{v}}_j = \tilde{\mathbf{v}}_i = \frac{m_i \mathbf{v}_i + m_j \mathbf{v}_j}{m_i + m_j}, \tag{11}$$

a property also obtained by Lowe [14] after relaxation and before thermalization.

Using $\tilde{\mathbf{v}}_i$, a half-time-step velocity is obtained from half of the conservative-force acceleration (first part of velocity-Verlet scheme)

$$\mathbf{v}_i^{n+1/2} = \tilde{\mathbf{v}}_i + \frac{1}{2} \frac{1}{m_i} \mathbf{F}_i^C \Delta t, \tag{12}$$

where $\Delta\, t$ is time step, and $\mathbf{F}_i^C$ is the total conservative force evaluated from the particle position $\mathbf{r}_i^n$. The new-time-step particle position is updated

$$\mathbf{r}_i^{n+1} = \mathbf{r}_i^n + \mathbf{v}_i^{n+1/2}\Delta t. \tag{13}$$

At last, the new-time-step velocity is obtained from

$$\mathbf{v}_i^{n+1} = \mathbf{v}_i^{n+1/2} + \frac{1}{2}\frac{1}{m_i}\mathbf{F}_i^{C,n+1}\Delta t, \tag{14}$$

where $\mathbf{F}_i^{C,n+1}$ is evaluated at the new-time-step particle position $\mathbf{r}_i^{n+1}$.

Eq. (10) is an operator-splitting approach similar to that of Shardlow [15] where the particle velocities are solved implicitly and locally in a pairwise fashion instead over the entire domain. An important difference is that here the pairwise updating of the particle velocities is performed in N_s sweeps for all particle pairs. For macroscopic flow simulations, optimum accuracy can be obtained by an adaptive sweeping scheme following Whitehouse et. al. [21]. For every time step consecutively $N_s = 2^m$ and $N_s = 2^{m+1}$ sweeps are performed, with m increasing until the relative error between the evaluated velocities is less then a specific dimensionless tolerance ε. The last calculated velocity is adopted and at the next time step the index m is decreased by one. It is found that a tolerance $\varepsilon = 5 \times 10^{-3}$ gives a good compromise between computational efficiency and accuracy. Note that the relaxed viscous stability on one hand allows for large time-step sizes, on the other hand may increase the temporal truncation error for large time-step sizes. For mesoscopic flow simulations, it is difficult to specify discrete tolerance ε *a priori*. For such cases our numerical experiments, as also will be shown in next sections, suggest that a fixed parameter $N_s = 5$ is sufficient to achieve Sc up to order $O(10^6)$.

4. Validation tests

The splitting scheme is tested by macroscopic Poiseuille and Couette flows and a mesoscopic temperature control test. For the macroscopic cases, the overall accuracy is measured by using an L_1-norm error defined as

$$L_1 = \frac{\sum_{i=1}^{N}\left|U_i^{th} - U_i^{SPH}\right|}{\sum_{i=1}^{N}\left|U_i^{th}\right|}, \tag{15}$$

where U_i^{th}, U_i^{SPH} are the theoretical and the simulated velocity fields evaluated at the particle positions $\mathbf{r}_i$, and N is the total number of particles. For the mesoscopic case the accuracy of the splitting scheme is measured by the difference between the measured kinetic temperature of the SDPD particle and the input value. Another validation, which is considered as an important issue in DPD [22], is the qualitative comparison between the computed radial distribution functions (RDF) of the SDPD particles and that which is typically obtained for liquids.

4.1. Poiseuille flow

For the first macroscopic case we consider a Poiseuille flow between two walls at $y = 0$ and $y = L$. The flow is initially at rest and suddenly driven by a constant body force F parallel to the x-axis. Periodic boundary conditions are employed in the flow direction. The flow parameters are chosen as $F = 10^{-4}$, $L = 10^{-3}$, $\rho = 10^3$ and $\mu = 10^{-6}$, which gives a maximum velocity at steady state of $V_{max} = FL^2/\mu$. The Reynolds number is $\mathrm{Re} = Lv_{max}/\eta = 1.25 \times 10^{-2}$, which is typical for micro-fluidic systems. A series of simulations are performed with increasing particle numbers $N_x = N_y = 10, 20, 40, 80$ (note that the particles initially are on a lattice), $\varepsilon = 5 \times 10^{-3}$ and time-step sizes ranging from $\Delta t = \Delta t_\mu = 7.8125 \times 10^{-5}$ to $16\Delta t_\mu$.

A comparison between the computed velocity profile with $N_y = 40$ and $\Delta t = 4\Delta t_\mu$ at time $t_m = 0.63$ and the theoretical solution is shown in Fig. 1(top). At this time the velocity profile is found to be very close to the steady state solution [18]. Fig. 2 (top) and Fig. 3(top) show the behavior of L_1-errors with increasing space and time resolution, which suggest at least first-oder convergence.

4.2. Couette flow

For the second macroscopic test case we consider a Couette flow between two walls at $y = 0$ and $y = L$, where one wall is at rest and the other is moving at constant speed V_0. Periodic boundary conditions are employed in the flow direction. The flow parameters are chosen as $\mu = 10^{-6}, V_0 = 1.25 \times 10^{-5}, L = 10^{-3}$ and $\rho = 10^3$, which gives a Reynolds number of $\mathrm{Re} = V_0 L/\mu = 1.25 \times 10^{-2}$ as in the first case. Similarly as in the first case, a series of simulations are performed with $N_x = N_y = 10, 20, 40, 80, \varepsilon = 5 \times 10^{-3}$ and time-step sizes ranging from $\Delta t = \Delta t_\mu = 7.8125 \times 10^{-5}$ to $16\Delta t_\mu$.

The comparison between SPH and the analytical solution of the velocity at time instant $t_m = 0.06$ is shown in Fig. 1 (bottom). The L_1-norm errors at $t_m = 0.06$ are shown in Fig. 2 (bottom) and Fig. 3 (bottom). Again, first-order convergence is obtained.

4.3. Temperature control of SDPD fluid

A mesoscopic box of fluid is considered. The simulation parameters are $k_B T = 1$, box size is $L = 1.25$, density $\rho = 1$, number of particles $N = 15 \times 15 \times 15 = 3375$, which give the input average thermal velocity $v_{kin}^i = \sqrt{3k_B T/m}$, where m is mass of a

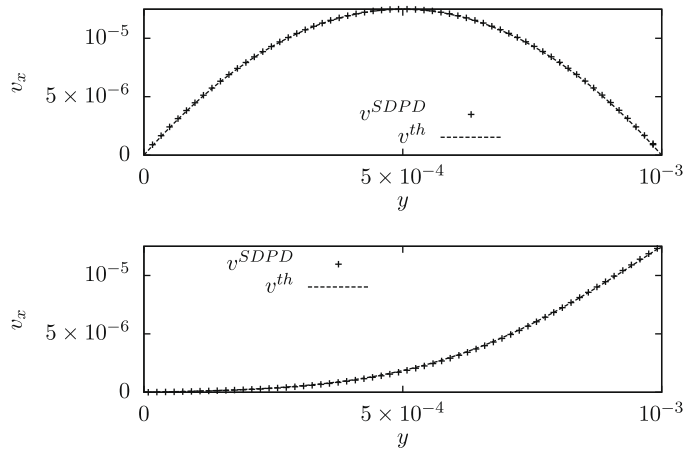

Fig. 1. Comparison of SPH and theoretical solutions for the Poiseuille flow (top) and the Couette flow (bottom) at time $t_m = 0.63$ and $t_m = 0.06$, respectively ($N_y = 40, \Delta t = 4\Delta t_\mu$).

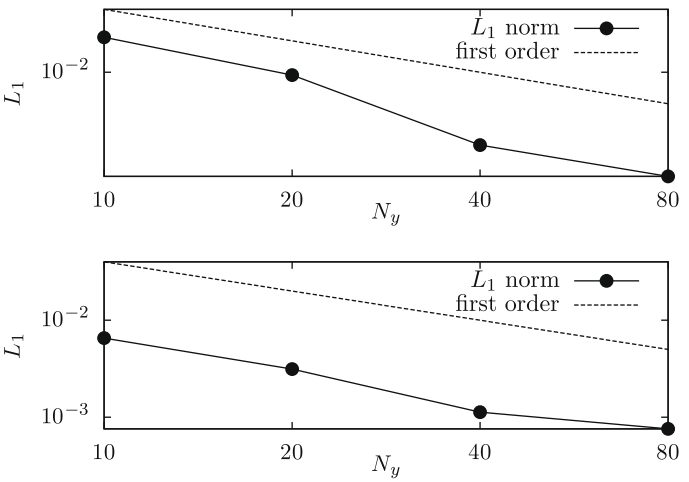

Fig. 2. Comparison of the L_1-norm error for the Poiseuille flow (top) and Couette flow (bottom) as a function of $N_y (\Delta t = 4\Delta t_\mu)$.

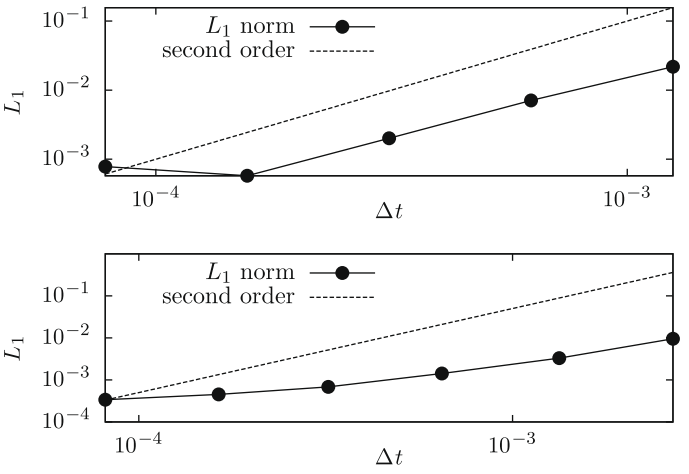

Fig. 3. Comparison of the L_1-norm error for the Poiseuille flow (top) and Couette flow (bottom) as a function of $\Delta t (N_y = 40)$.

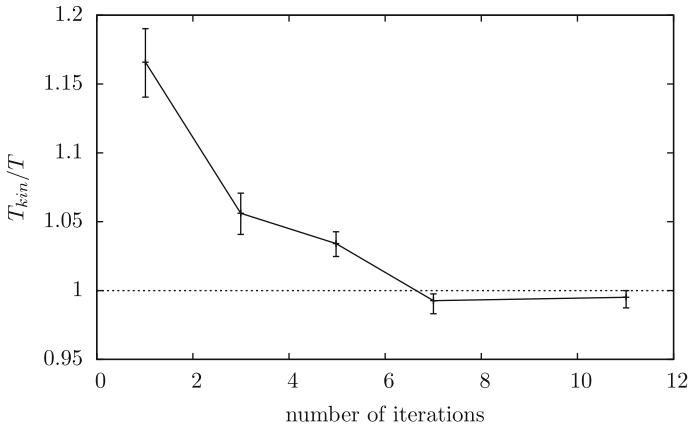

Fig. 4. Difference between the measured averaged kinetic temperature (solid line) and the input temperature (dash line) with increasing number of sweeps.

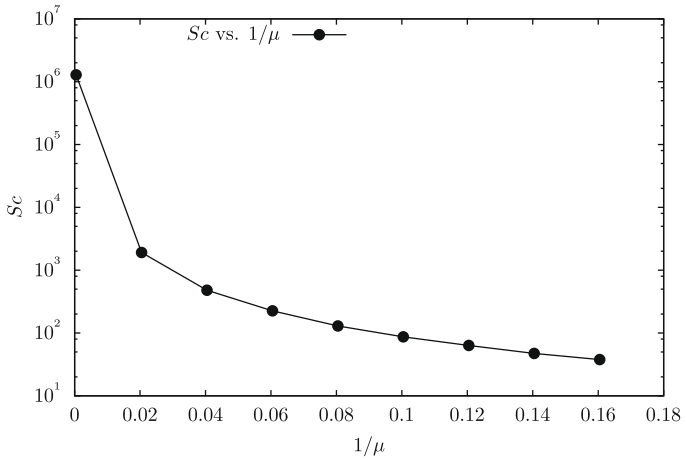

Fig. 5. Relation between the computed Schmidt number of the SDPD fluid and the inputed viscosity (the inversed values is shown on *x* axis).

particle. In order to study the potential of the splitting scheme a large range of viscosities, from $\mu = 6.25$ to 2.2×10^3, has been used. The time step used is based on the CFL condition and kept constant for all simulations. To obtain Sc from Eq. (1), the self-diffusion coefficient is measured by fitting the mean-square displacement of the particles.

The relation of the number of sweeps N_s to the predicted kinetic temperature $T_{kin} = m v^s_{kin^2}/3k_B$, where v^s_{kin} is the average thermal velocity of the particles, for the maximum input viscosity $\mu = 2.2 \times 10^3$ is shown in Fig. 4.

It is found that the measured kinetic temperature converges to the input value T_{th} with increasing N_s. Note that reasonably small errors below 5% are achieved with $N_s = 5$, where the total computational effort increases by less than 20%. Further numerical experiments show that even fewer N_s sweeps are required for accurate temperature control at smaller viscosities. The relation between Sc and the input viscosity is shown in Fig. 5, suggesting that a Sc of order $O(10^6)$ has been achieved.

The computed RDF of the SDPD particles is shown in Fig. 6, which is not affected by the implicit treatment of the viscous terms and preserves the shape typical for liquids.

5. Polymer in simple shear flow

In this case, the effect of Sc on a polymer chain in simple shear flow is studied. A mesoscopic box of fluid with a 5-bead free polymer in simple shear is considered similarly as in [12]. The polymer is modeled by a chain of double-linked beads [9] which have all properties of SDPD particles, and additionally are subjected to interaction forces with neighboring polymer beads according to the FENE potential

$$U_{FENE} = -\frac{1}{2} k R_0^2 ln\left[1 - \left(\frac{r}{R_0}\right)^2\right], \tag{16}$$

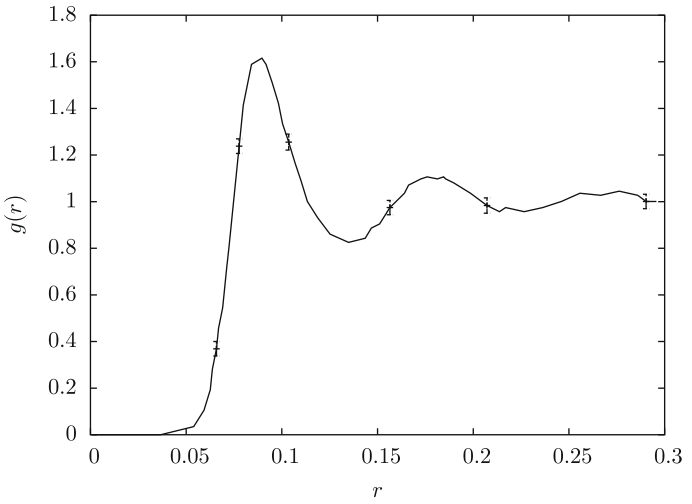

Fig. 6. Computed radial distribution function for the SDPD fluid with $\mu = 2.2 \times 10^3$ and Sc number of order $O(10^6)$.

Table 1
Gyration radius of a free polymer in static solution and in simple shear flow.

Sc	1.225×10^3	2.5×10^3	2.5×10^5	1.0×10^6
$\langle R_g \rangle$	0.0048	0.0052	0.0048	0.0048
$\langle R_g^{\text{flow}} \rangle$	0.0057	0.0058	0.0092	0.0120

where r is the distance between neighboring beads, R_0 is the maximum spring extension, and k is the spring constant. This model of polymer in suspension produces correct scaling laws for static and dynamic properties, see [9] for further details. Other simulation parameters are $k_BT = 1$, box size $L = 0.75$, mass density $\rho = 1$, shear rate $\dot{\gamma} = 0.5$ and number of particles $N = 15 \times 15 \times 15 = 3375$. Periodic boundary conditions are employed in the flow direction and the spanwise direction, and a Lees–Edwards boundary condition [23] is applied at the upper and lower boundaries.

Table 1 summarizes the relations between the values of Sc and gyration radius of a free polymer in static solution $\langle R_g \rangle$ and in a simple shear flow $\langle R_g^{\text{flow}} \rangle$.

It is found that the average size of the polymer in static fluid is nearly independent of Sc. However, when the polymer is in a shear flow, its gyration radius increases dramatically with Sc of the solvent, which is in good agreement with the results of [12].

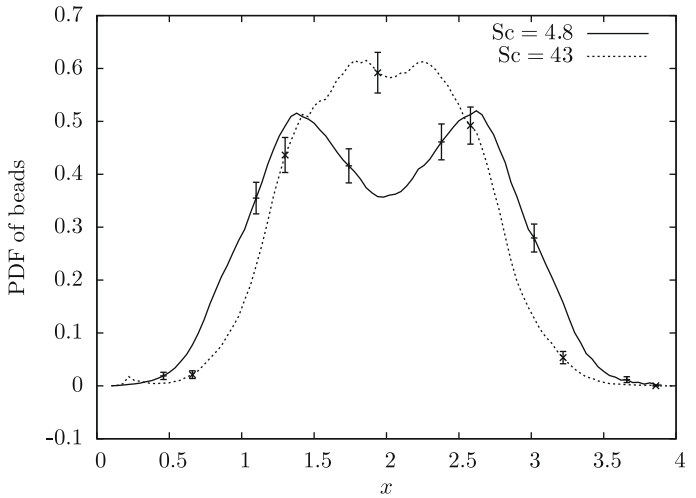

Fig. 7. Effect of Sc on the polymer density profile in Poiseuille flow, where $x = 0$ and 4 correspond the channel walls, for the cases Sc = 4.8 and 43, respectively.

6. Polymer in Poiseuille flow

The SDPD simulation of a polymer in a Poiseuille flow is set up in a box with dimensions $L_x \times L_y \times L_z$, where $L_y = 4.0$, $L_z = 8.0$, and $L_x = 4.0$ is the distance between the walls (at $y = 0$ and $y = L_y$). The flow is driven by a body force in the direction of the z axis. Periodic boundary conditions are employed in the flow direction and the spanwise direction. The number of particles is $N_x \times N_y \times N_z = 10 \times 10 \times 20$, and 20 of them were connected to form a polymer in dilute solution. To illustrate the effect on the distribution of the polymer beads in the channel two simulations are performed with Sc of 4.8 and 43, respectively. The spanwise distribution of polymer mass is shown in Fig. 7. It is found that the depletion region at the center of the channel is more pronounced with low Sc, and the polymer concentration tends to be higher in the center with smaller off-center peaks with high Sc. These results are in agreement with those in the recent study of Millan and Laradji [24], and suggest a strong influence of Sc on the polymer behavior in a shear flow.

7. Concluding remarks

We have developed a splitting scheme for highly dissipative smoothed particle dynamics. In the time-splitting part of the scheme, the contribution of the conservative force is updated separately from that of the dissipative and random forces. In the operator-splitting part of the scheme the particle velocities are updated by sweeping over all particle pairs within the domain in a pairwise fashion with an explicit/implicit two-step algorithm. The number of sweeps in the present scheme is adjusted adaptively to achieve higher accuracy. Numerical experiments show that the present scheme has a great potential in addressing realistic dissipative mesoscopic flow problems without significantly increasing the computational effort.

References

[1] J.J. Monaghan, Smoothed particle hydrodynamics, Rep. Prog. Phys. 68 (8) (2005) 1703–1759.
[2] P. Español, M. Revenga, Smoothed dissipative particle dynamics, Phys. Rev. E 67 (2) (2003) 26705.
[3] X. Hu, N. Adams, A multi-phase SPH method for macroscopic and mesoscopic flows, J. Comput. Phys. 213 (2) (2006) 844–861.
[4] P. Hoogerbrugge, J. Koelman, Simulating microscopic hydrodynamic phenomena with dissipative particle dynamics, Europhys. Lett. 19 (3) (1992) 155–160.
[5] V. Symeonidis, G.E. Karniadakis, B. Caswell, Dissipative particle dynamics simulations of polymer chains: scaling laws and shearing response compared to DNA experiments, Phys. Rev. Lett. 95 (7) (2005) 76001.
[6] V. Symeonidis, G.E. Karniadakis, A family of time-staggered schemes for integrating hybrid dpd models for polymers: algorithms and applications, J. Comput. Phys. 218 (1) (2006) 82–101.
[7] E.A.J.F. Peters, Elimination of time step effects in DPD, Europhys. Lett. 66 (3) (2004) 311–317.
[8] W.H. Jiang, J.H. Huang, Y.M. Wang, M. Laradji, Hydrodynamic interaction in polymer solutions simulated with dissipative particle dynamics, J. Chem. Phys. 126 (4) (2007) 44901.
[9] S. Litvinov, M. Ellero, X. Hu, N. Adams, Smoothed dissipative particle dynamics model for polymer molecules in suspension, Phys. Rev. E 77 (6) (2008) 66703.
[10] A. Vázquez-Quesada, M. Ellero, P. Español, Consistent scaling of thermal fluctuations in smoothed dissipative particle dynamics, J. Chem. Phys. 130 (2009) 034901.
[11] R.D. Groot, P.B. Warren, Dissipative particle dynamics: bridging the gap between atomistic and mesoscopic simulation, J. Chem. Phys. 107 (11) (1997) 4423–4435.
[12] V. Symeonidis, G. Karniadakis, B. Caswell, Schmidt number effects in dissipative particle dynamics simulation of polymers, J. Chem. Phys. 125 (2006) 184902.
[13] I. Pagonabarraga, M. Hagen, D. Frenkel, Self-consistent dissipative particle dynamics algorithm, Europhys. Lett. 42 (4) (1998) 377–382.
[14] C. Lowe, An alternative approach to dissipative particle dynamics, Europhys. Lett. 47 (1999) 145–151.
[15] T. Shardlow, Splitting for dissipative particle dynamics, SIAM J. Sci. Comput. 24 (4) (2003) 1267–1282.
[16] P. Nikunen, M. Karttunen, I. Vattulainen, How would you integrate the equations of motion in dissipative particle dynamics simulations?, Comput Phys. Commun. 153 (3) (2003) 407–423.
[17] J. Monaghan, Implicit SPH drag and dusty gas dynamics, J. Comput. Phys. 138 (2) (1997) 801–820.
[18] J.P. Morris, P.J. Fox, Y. Zhu, Modeling low Reynolds number incompressible flows using sph, J. Comput. Phys. 136 (1) (1997) 214–226.
[19] M. Grmela, H. Öttinger, Dynamics and thermodynamics of complex fluids. I: Development of a general formalism, Phys. Rev. E 56 (6) (1997) 6620–6632.
[20] H. Öttinger, M. Grmela, Dynamics and thermodynamics of complex fluids. II: Illustrations of a general formalism, Phys. Rev. E 56 (6) (1997) 6633–6655.
[21] S. Whitehouse, M. Bate, Smoothed particle hydrodynamics with radiative transfer in the flux-limited diffusion approximation, Mon. Not. R. Astron. Soc. 353 (4) (2004) 1078–1094.
[22] F. Thalmann, J. Farago, Trotter derivation of algorithms for brownian and dissipative particle dynamics, J. Chem. Phys. 127 (12) (2007) 124109.
[23] A. Lees, S. Edwards, The computer study of transport processes under extreme conditions, J. Phy. C: Solid State Phys. 5 (1972) 1921–1928.
[24] J.A. Millan, M. Laradji, Cross-stream migration of driven polymer solutions in nanoscale channels: a numerical study with generalized dissipative particle dynamics, Macromolecules 42 (3) (2009) 803–810.